International Journal of Theoretical and Applied Mathematics
2023; 9(3): 23-34
http://www.sciencepublishinggroup.com/j/ijtam
doi: 10.11648/j.ijtam.20230903.11
ISSN: 2575-5072 (Print); ISSN: 2575-5080 (Online)

Analyzing Steady State Heat and Mass Transfer in Jeffrey Nanofluid with Nonlinear Thermal Radiation

Michael Williams[1, *], Isah Bala Yabo[1], Aminu Mustafa[1], Ahmed Audu[2]

[1]Department of Mathematics, Usmanu Danfodiyo University, Sokoto, Nigeria

[2]Department of Statistics, Usmanu Danfodiyo University, Sokoto, Nigeria

Email address:

michealwilliams185@gmail.com (Michael Williams)

[*]Corresponding author

To cite this article:

Michael Williams, Isah Bala Yabo, Aminu Mustafa, Ahmed Audu. (2023). Analyzing Steady State Heat and Mass Transfer in Jeffrey Nanofluid with Nonlinear Thermal Radiation. *International Journal of Theoretical and Applied Mathematics*, *9*(3), 23-34. https://doi.org/10.11648/j.ijtam.20230903.11

Received: October 7, 2023; **Accepted**: October 23, 2023; **Published**: December 22, 2023

Abstract: The steady state magnetohydrodynamic flow of Jeffrey nanofluid with nonlinear thermal radiation, over a porous plate together with prescribed boundary conditions of interest was carried out via Lie symmetry group alteration. The all-inclusive flow of the present model incorporates the Jeffrey parameters, nonlinear thermal radiation, heat generation, Brownian motion, chemical reaction, thermophoresis and porosity parameter. The derived governing equations of the problem are highly nonlinear coupled partial differential equations. The Lie group approach was used to convert the system partial differential equations to a system of ordinary differential equations which was solved numerically with the help of a matlab solver called bvp4c. The established numerical results were discussed with help of line graph. The Rayleigh number and porosity parameter enriched the velocity fluid. The rise of the temperature ratio parameter and heat generation parameter improved the temperature contours and is reduced by boosting the Prandtl number. Lewis number, chemical reaction parameter diminished the concentration profile and took the opposite direction for Biot number. Equally, by improving Jeffrey parameter and Hartmann number weakened skin friction profile. Also, Sherwood number, and the Nusselt number were also expanded. The recent outcome will be useful in the automobile industry, polymer industry and so on.

Keywords: Nonlinear Thermal Radiation, Heat Source-Sink, Porosity Parameter and Jeffrey Parameter

1. Introduction

So many researchers' attention has been drowned on nonlinear thermal radiation as a result of its application in engineering works. However, nonlinear thermal radiation is very significant in processing industries that make use of heat to obtain a good end product. This end product can be used to produce gas turbines and plants for electricity generation etc. [1]. Scrutinized the consequence of Maxwell nanoliquid on a parallel plate using chemical reaction and linear thermal radiation. In addition, their upshot is used in the boosting transfer of heat, energy derived from solar, structures of transportation, and so on. [2]. Carried out the significance of nonlinear thermal radiation and thermophoresis on a heat and mass transfer of a mixed convective vertical channel. The fluid temperature is improved by raising the values of radiative heat flux which in turn causes the velocity and concentrations close to the porous surface to go up. [3]. Carried out the importance of nonlinear thermal radiation in a Walter-B nanofluid by making use of thermophoresis, Brownian motion, and convective boundary conditions. Their outcome shows that escalating the Schmidt number reduced the concentration of nanofluid. [4]. Investigated the magnetohydrodynamic transfer of heat on a parallel plate. Their outcome exposed how the transfer of heat and fluid flow upset the leading surface.

A nanofluid is a based fluid and nanoparticles which is a class of fluid for heat transfer. The heat and mass transfer performance is improved by the base fluid. Today's refrigerating rate requests to meet the thermal conductivity of the ordinary heat transfer liquids is inadequate. Nanofluids have been exposed to upturn the convective and thermal conductivity heat and mass transfer performance of the base

fluids. Brownian motions of the nanoparticles inside the base fluids are one of the likely devices for unusual growth in the thermal conductivity of nanofluids. A diversity of nuclear reactor projects introduced by improved safety and better economics are being planned by the nuclear power industry everywhere to more accurately solve the impending energy supply deficit. Nanoliquids are suspensions of nanoparticles in fluids that show important improvement of their possessions at modest nanoparticle concentrations. The industrial applications of nanofluids include biomedicine, food, transportation, nuclear reactors and electronics. Although, in nuclear reactors, forced convection is used to remove heat from fuel elements which makes it more significant in heat transfer procedure. Also, nanofluids have an advanced viscosity which agrees to an upsurge in driving power and display better heat transfer properties than pure materials. Electronic applications which use microfluidic applications also make use of nanofluids. Some analysis of nanofluids can be seen in the studies [5-11].

In addition, Jeffrey fluid is non- Newtonian fluid which has numerous applications in engineering processes. The multiplicity in physical nature of these fluids leads to the expansion of diverse constitutive dealings because all the features cannot be discovered through one relation. According to the experts such materials can be divided into three groups such as, integral, differential and rate types. The agreed model is called Jeffrey fluid which fits to the group of rate type materials. Such materials forecast the retardation/ relaxation times features. Several investigations on this model can be perceived [12-16].

Nevertheless, automotive industries, nuclear reactors, and transformers make use of porous material which has attracted so many researchers. [17]. Deliberated on the Darcy model for porous medium with Jeffrey nanofluid that was used as a based fluid. [18]. Explore magnetohydrodynamic (MHD) with thermal radiation and porous medium on a convective Jeffrey nanofluid flow. [19]. Illustrated convective heating conditions on the flow of Jeffrey nanofluids with combined porous and magnetic effects.

This recent work intends to improve the work of [1] by incorporating Jeffrey parameters and porous material, nonlinear thermal radiation and heat generation. Also, the Lie symmetry group was used to alter the system of partial differential equations into ordinary differential equations and a matlab solver called bvp4c was used to solve numerically.

2. Modeling

The flow of Jeffrey nanofluid in a stretching porous sheet with nonlinear thermal radiation and heat generation was formulated. The permeable parallel plate creates the flow. Brownian motion and Thermophoresis were also considered. From figure 1, the fluid is assumed to flow in x-direction.

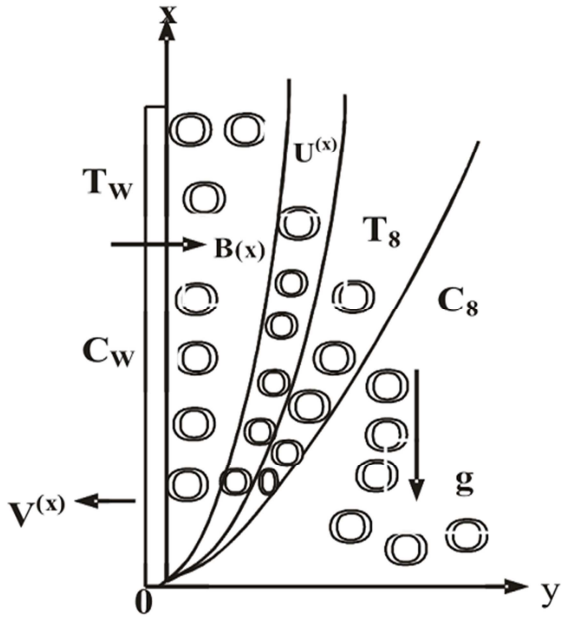

Figure 1. *Coordinating system for the porous media.*

The governing expressions are as [1, 22]:

$$\frac{\partial u}{\partial x}+\frac{\partial v}{\partial y}=0 \tag{1}$$

$$u\frac{\partial u}{\partial x}+v\frac{\partial u}{\partial y}+\frac{\lambda_1}{1+\lambda}\left[u^2\frac{\partial^2 u}{\partial x^2}+v^2\frac{\partial^2 u}{\partial y^2}+2uv\frac{\partial^2 u}{\partial x\partial y}\right]=$$

$$\frac{V}{1+\lambda}\frac{\partial^2 u}{\partial y^2}+\left[(1-C_\infty)\rho_{f_\infty}\beta(T-T_\infty)-\left(\rho_p-\rho_{f_\infty}\right)(C-C_\infty)\right]g-\frac{\sigma B^2(x)}{\rho_f}\left[u+\lambda_1 vu\frac{\partial u}{\partial y}\right]-\frac{1}{K}u \tag{2}$$

$$u\frac{\partial T}{\partial x}+v\frac{\partial T}{\partial y}=\frac{\kappa}{\rho c_p}\frac{\partial^2 T}{\partial y^2}-\frac{1}{\rho c_p}\frac{\partial q_r}{\partial y}+\frac{Q_0}{\rho c_p}(T-T_\infty)+\tau\left[D_B\frac{\partial C}{\partial y}\frac{\partial T}{\partial y}+\frac{D_T}{T_\infty}\left(\frac{\partial T}{\partial y}\right)^2\right] \tag{3}$$

$$u\frac{\partial C}{\partial x}+v\frac{\partial C}{\partial y}=D_B\frac{\partial^2 C}{\partial y^2}+\frac{D_T}{T_\infty}\frac{\partial^2 T}{\partial y^2}-R(C-C_\infty) \tag{4}$$

The boundary conditions for the above models are as [1]:

$$\left.\begin{aligned} &u = U_w(x) = C_1 xv = v_w(x), T = \frac{-k\partial T}{\partial y} = hf\left(T_f - T\right), C = C_w aty = 0 \\ &u \to 0, T \to T_{\infty,} C \to C_\infty asy \to \infty \end{aligned}\right\} \tag{5}$$

To streamline the radiative heat flux in this work Rosseland approximation is used

$$q_r = -\frac{4\sigma_1}{3k_1}\frac{\partial T^4}{\partial y} \tag{6}$$

In order to linearize equation (6), expand T^4 about T_∞ into Taylor's series expansion gives

$$T^4 = \left(\frac{T - T_\infty}{T_w - T_\infty}\left(T_1 - T_0\right) + T_0\right)^4 \tag{7}$$

The following emerged by putting equations (6-7) into equation (3)

$$u\frac{\partial T}{\partial x} + v\frac{\partial T}{\partial y} = \left[1 + \frac{4N}{3}\left(C_T + \frac{T - T_\infty}{T_w - T_\infty}\right)^3\right]\frac{\partial^2 T}{\partial y^2} + 4N\left[C_T + \frac{T - T_\infty}{T_w - T_\infty}\right]^2\left(\frac{\partial T}{\partial y}\right)^2$$

$$+\frac{Q_0}{\rho c_p}(T - T_\infty) + \tau\left[D_B\frac{\partial C}{\partial y}\frac{\partial T}{\partial y} + \frac{D_T}{T_\infty}\left(\frac{\partial T}{\partial y}\right)^2\right] \tag{8}$$

The stream function is defined as follows:

$$v = -\frac{\partial \psi}{\partial x} and, u = \frac{\partial \psi}{\partial y} \tag{9}$$

Together with non- dimensional variables

$$\left.\begin{aligned} &\theta = \frac{T - T_\infty}{T_w - T_\infty}, \phi = \frac{C - C_\infty}{C_w - C_\infty}, \Pr = \frac{\mu\rho c_p}{\kappa}, M = \frac{\sigma B_0^2}{\rho_f}, Ra = \frac{(1 - \phi_\infty)\beta g\Delta\theta}{V}, \\ &Le = \frac{\alpha}{D_b}, Nr = \frac{\left(\rho_p - \rho_{f_\infty}\right)\Delta\phi}{\rho_{f_\infty}\beta\Delta\theta(1 - \phi_\infty)}, Nb = \frac{D_B\Delta\phi(\rho c)_p}{\kappa}, Nt = \frac{D_T\Delta\theta(\rho c)_p}{\kappa T_\infty}, K = \frac{v_\infty}{bk}, \\ &N = \frac{4T_\infty^3\sigma_1}{\mathrm{K}_1\kappa}, \gamma = \frac{Uk}{D_B}, \beta = \lambda_1 C_1, Q = \frac{Q_0}{\rho c_p}, x = \frac{C_1}{U_1}x, y = \sqrt{\frac{C_1}{v}}y, u = \frac{u}{U_1} \end{aligned}\right\} \tag{10}$$

The equations below emerged by putting equations (9 - 10) into equations (1 -5) and equation (8).

$$(1 + \lambda)\left[\frac{\partial \psi}{\partial y}\frac{\partial^2 \psi}{\partial x \partial y} - \frac{\partial \psi}{\partial x}\frac{\partial^2 \psi}{\partial y^2}\right] + \beta\left[\left(\frac{\partial \psi}{\partial y}\right)^2\frac{\partial^3 \psi}{\partial x^2 \partial y} - \left(\frac{\partial \psi}{\partial x}\right)^2\frac{\partial^3 \psi}{\partial y^3} - 2\frac{\partial \psi}{\partial y}\frac{\partial \psi}{\partial x}\frac{\partial^3 \psi}{\partial x \partial y^2}\right] =$$

$$\frac{\partial^3 \psi}{\partial y^3} + (1 + \lambda)Ra[\theta - N_r\phi] - (1 + \lambda)M\left(\frac{\partial \psi}{\partial y} - \beta\frac{\partial \psi}{\partial x}\frac{\partial^2 \psi}{\partial y^2}\right) - (1 + \lambda)\frac{1}{K}\frac{\partial \psi}{\partial y} \tag{11}$$

$$\Pr\left[\frac{\partial\psi}{\partial y}\frac{\partial\theta}{\partial x}-\frac{\partial\psi}{\partial x}\frac{\partial\theta}{\partial y}\right]=\left[1+\frac{4N}{3}\left(C_T+\theta\right)^3\right]\frac{\partial^2\theta}{\partial y^2}+4N\left[C_T+\theta\right]^2\left(\frac{\partial\theta}{\partial y}\right)^2+Q\theta+N_b\frac{\partial\phi}{\partial y}\frac{\partial\theta}{\partial y}+N_t\left(\frac{\partial\theta}{\partial y}\right)^2 \tag{12}$$

$$Le\left[\frac{\partial\psi}{\partial y}\frac{\partial\phi}{\partial x}-\frac{\partial\psi}{\partial x}\frac{\partial\phi}{\partial y}\right]=\frac{\partial^2\phi}{\partial y^2}+\frac{N_t}{N_b}\frac{\partial^2\theta}{\partial y^2}-\gamma\phi \tag{13}$$

The following boundary conditions emerged

$$\left.\begin{aligned}&\frac{\partial\psi}{\partial y}=x,-\frac{\partial\psi}{\partial x}=\frac{V_w}{\sqrt{C_1 v}},\theta=-B_i\left(1-\theta\right),\phi=1aty=0\\&\frac{\partial\psi}{\partial y}\to 0,?\theta\to 0,\phi\to 0asy\to\infty\end{aligned}\right\} \tag{14}$$

Table 1 show the explanations of symbols

Table 1. *Nomenclature.*

Description	Symbol	Description	Symbol
Biot number	Bi	Hartmann number	M
Heat source/sink	Q	Lewis number	Le
Similarity variable	η	Brownian motion parameter	Nb
Transverse magnetic field	$B(x)$	Thermal radiation parameter	N
Magnetic field strength	B_0	Density of base fluid	ρ_f
Velocity components along x, y-axis	u,v	Temperature variable	T
Nanoparticles specific heat	$(\rho c)_p$	Ambient liquid concentration	C_∞
Heat capacity ratio	τ	Stefan-Boltzmann constant	σ_1
Nanoparticles concentration	C	Non-uniform heat generation	Q_0
Mean absorption coefficient	K^*	Absorption coefficient	k_1
Ambient liquid temperature	T_∞	Rayleigh number	Ra
Fluid specific heat at constant pressure	$(\rho c)_f$	Prandtl number	Pr
Deborah number	β	Temperature ratio	Ct
Mass transfer parameter	S	Thermal conductivity	κ
Brownian diffusion	D_B	Termophretic diffusion	D_T
Specific heat at constant pressure	C_1	Porous material	K
Free stream velocity of the flow	U	Reference concentration	C_w
Reference temperature	T_w	Gravitational acceleration	g
Dimensionless velocity	f	Fluid specific heat	$(\rho c)_f$
Velocity of the exterior stream	$U(x)$	Thermophoresis parameter	Nt
Condition far away from the plate	v_∞	Constant	b
Chemical reaction parameter	γ	Electrical conductivity	σ
Kinematic viscosity	ν	Jeffrey parameter	λ
Relaxation time	λ_1	Buoyancy ratio	Nr
Stream function	ψ	Dimensionless temperature	θ
Dimensionless concentration	ϕ	Thermal diffusivity	α
Volumetric thermal expansion coefficient of the base fluid	δ	The fluid viscosity	μ

2.1. Lie Symmetry Group

Using the standard Lie group approach [1, 11]. for scaling alteration group are introduced below where ε is the parameter of the group and α is the real number.

$$\Gamma: x^*=xe^{\varepsilon\alpha_1},y^*=ye^{\varepsilon\alpha_2},\psi^*=\psi e^{\varepsilon\alpha_3},\theta^*=\theta e^{\varepsilon\alpha_4},\phi^*=\phi e^{\varepsilon\alpha_5} \tag{15}$$

Substituting equation (15) into equation (11) – (13) we get:

$$e^{\varepsilon\left(2\alpha_2+\alpha_1-2\alpha_3\right)}(1+\lambda)\left[\frac{\partial\psi^*}{\partial y^*}\frac{\partial^2\psi^*}{\partial x^*\partial y^*}-\frac{\partial\psi^*}{\partial x^*}\frac{\partial^2\psi^*}{\partial y^{*2}}\right]+$$

$$\beta e^{\varepsilon\left(2\alpha_1+3\alpha_2-3\alpha_3\right)}\left[\left(\frac{\partial\psi^*}{\partial y^*}\right)^2\frac{\partial^3\psi^*}{\partial x^{*2}\partial y^*}+\left(\frac{\partial\psi^*}{\partial x^*}\right)^2\frac{\partial^3\psi^*}{\partial y^{*3}}-2\frac{\partial\psi^*}{\partial y^*}\frac{\partial\psi^*}{\partial x^*}\frac{\partial^3\psi^*}{\partial x^*\partial y^{*2}}\right]$$

$$=e^{\varepsilon\left(3\alpha_2-\alpha_3\right)}\frac{\partial^3\psi^*}{\partial y^{*3}}+e^{-\varepsilon\alpha_4}\left[(1+\lambda)Ra\theta^*\right]-e^{-\varepsilon\alpha_5}\left[(1+\lambda)RaN_r\phi^*\right]-$$

$$(1+\lambda)M^2\left[e^{\varepsilon\left(\alpha_2-\alpha_3\right)}\frac{\partial\psi^*}{\partial y^*}-e^{\varepsilon\left(\alpha_1+2\alpha_2-2\alpha_3\right)}\beta\frac{\partial\psi^*}{\partial x^*}\frac{\partial^2\psi^*}{\partial y^{*2}}\right]-e^{\varepsilon\left(\alpha_2-\alpha_3\right)}(1+\lambda)\frac{1}{K}\frac{\partial\psi^*}{\partial y^*} \tag{16}$$

$$e^{\varepsilon\left(\alpha_1+\alpha_2-\alpha_3-\alpha_4\right)}\Pr\left[\frac{\partial\psi^*}{\partial y^*}\frac{\partial\theta^*}{\partial x^*}-\frac{\partial\psi^*}{\partial x^*}\frac{\partial\theta^*}{\partial y^*}\right]=e^{\varepsilon\left(2\alpha_2-4\alpha_4\right)}\left[1+\frac{4}{3}N\left(C_T-\theta^*\right)^3\right]\frac{\partial^2\theta^*}{\partial y^{*2}}+$$

$$e^{\varepsilon\left(2\alpha_2-4\alpha_4\right)}4N\left[C_T+\theta^*\right]^2\left(\frac{\partial\theta^*}{\partial y^*}\right)^2+e^{\varepsilon\left(-\alpha_4\right)}Q\theta^*+e^{\varepsilon\left(2\alpha_2-\alpha_4-\alpha_5\right)}N_b\frac{\partial\phi^*}{\partial y^*}\frac{\partial\theta^*}{\partial y^*}+e^{\varepsilon\left(2\alpha_2-2\alpha_4\right)}N_t\left(\frac{\partial\theta^*}{\partial y^*}\right)^2 \tag{17}$$

$$e^{\varepsilon\left(\alpha_1+\alpha_2-\alpha_3-\alpha_5\right)}Le\left[\frac{\partial\psi^*}{\partial y^*}\frac{\partial\phi^*}{\partial x^*}-\frac{\partial\psi^*}{\partial x^*}\frac{\partial\phi^*}{\partial y^*}\right]=e^{\varepsilon\left(2\alpha_2-\alpha_5\right)}\frac{\partial^2\phi^*}{\partial y^{*2}}+e^{\varepsilon\left(2\alpha_2-\alpha_4\right)}\frac{N_t}{N_b}\frac{\partial^2\theta^*}{\partial y^{*2}}-e^{-\varepsilon\left(\alpha_5\right)}\gamma\phi^* \tag{18}$$

Through equating different exponential expressions of equations (16) - (18) the invariant of the method emerged

$$\left.\begin{aligned}&2\alpha_2+\alpha_1-2\alpha_3=2\alpha_1+\alpha_2-3\alpha_3=3\alpha_2-\alpha_3=-\alpha_4=-\alpha_5=\alpha_2-\alpha_3=\alpha_1+2\alpha_2-2\alpha_3=\alpha_2-\alpha_3\\&\alpha_1+\alpha_2-\alpha_3-\alpha_4=2\alpha_2-4\alpha_4=2\alpha_2-4\alpha_4=-\alpha_4=2\alpha_2-\alpha_4-\alpha_5=2\alpha_2-2\alpha_4\\&\alpha_1+\alpha_2-\alpha_3-\alpha_5=2\alpha_2-\alpha_5=2\alpha_2-\alpha_4=-\alpha_5\end{aligned}\right\} \tag{19}$$

From equation (14) the invariance of the boundary conditions becomes

$$\alpha_1=\alpha_3,\ \ \alpha_2=\alpha_4=\alpha_5=0 \tag{20}$$

Focus to the results of equation (19) applying equation (20) the group alterations (15) becomes:

$$\left.\Gamma: x^*=xe^{\varepsilon\alpha_1},y^*=y,\psi^*=\psi e^{\varepsilon\alpha_1},\theta^*=\theta,\phi^*=\phi\right\} \tag{21}$$

Also, employing Taylor series expansions yields

$$\left.\begin{aligned}&x^*-x=\varepsilon x\alpha_1+0(\varepsilon^2)\\&y^*-y=0\\&\psi^*-\psi=\varepsilon\psi\alpha_1+0(\varepsilon^2)\\&\theta^*-\theta=0\\&\phi^*-\phi=0\end{aligned}\right\} \tag{22}$$

Since $\alpha_1\neq 0$, rewriting equation (22) the following emerged

$$\left.\frac{x^*-x}{x\alpha_1}=\varepsilon, y^*-y=0, \frac{\psi^*-\psi}{\psi\alpha_1}=\varepsilon, \theta^*-\theta=0, \phi^*-\phi=0\right\} \tag{23}$$

Now, in terms of differentials equation (23) becomes

$$\frac{d\psi^*}{\alpha_1\psi^*}=\frac{dx^*}{x^*\alpha_1} \tag{24}$$

$$dy^*=d\theta^*=d\phi^*=0 \tag{25}$$

The similarity below is achieved through integrating equation (24) – (25)

$$\left.y^*=\eta, \psi^*=x^* f(\eta), \theta^*=\theta(\eta) and \phi^*=\phi(\eta)\right\} \tag{26}$$

Where η, $f(\eta)$, $\theta(\eta)$, and $\phi(\eta)$ are constant

The below equations are achieved by substituting equation (26) into equations (11) – (14)

$$f'''+(1+\lambda)\left[ff''-f'^2\right]-\beta\left[f^2 f'''-2f'ff''\right]-(1+\lambda)\left[M^2\left(f'-\beta ff''\right)+\frac{1}{K}f'\right]+(1+\lambda)Ra[\theta-N_r\phi]=0 \tag{27}$$

$$\left[[\Pr]\left[1+\frac{4}{3}N\left(C_T+\theta\right)^3\right]\theta''+4N\left[C_T+\theta\right]^2\theta'^2+\left[f\theta'+Q\theta+N_b\phi'\theta'+N_t\theta'^2\right]\right]=0 \tag{28}$$

$$\phi''+\frac{N_t}{N_b}\theta''+Le\left[f\phi'-\gamma\phi\right]=0 \tag{29}$$

While the boundary conditions read:

$$\left.\begin{array}{l} f=S, f'=1, \theta'=-B_i(1-\theta), \phi=1 at \eta=0 \\ f'\to 0, \theta\to 0, \phi\to 0 as \eta\to\infty \end{array}\right\} \tag{30}$$

2.2. Physical Terms

The concerned physical terms are $\left(C_f\right)$, (Nur), and (Shr):

$$C_f=\frac{1}{2}\mathrm{Re}_x^{-1/2}C_f=f''(0) \tag{31}$$

$$Nur=\mathrm{Re}_x^{-1/2}Nu=-\theta'(0) \tag{32}$$

$$Shr=\mathrm{Re}_x^{-1/2}Sh=-\phi'(0) \tag{33}$$

2.3. Method of Computation

The following alteration was used to alter equations (27) – (29) into first order initial value problem

$$\left(h_1, h_2, h_3, h_4, h_5, h_6, h_7, h_8, h_9, h_{10}\right)=\left(f, f', f'', f''', \theta, \theta', \theta'', \phi, \phi', \phi''\right) \tag{34}$$

$$\begin{pmatrix} h_1 \\ h_2 \\ h_3 \\ h_4 \\ h_5 \\ h_6 \\ h_7 \end{pmatrix} = \begin{pmatrix} y_2 \\ y_3 \\ \left[\frac{1}{1-\beta y_1^2}\right]\left[-2\beta y_2 y_1 y_3-(1+\lambda)[y_1 y_3-y_2^2]+(1+\lambda)\left[M(y_2-\beta y_1 y_3)+\frac{1}{K}y_2\right]+(1+\lambda)Ra[y_4-Nry_6]\right] \\ y_5 \\ \frac{1}{\left[1+\frac{4}{3}N(C_T+y_4)^3\right]}\left[-4N(Ct+y_4)^2 y_5^2-Pr(y_1 y_5+Qy_4+Nby_7 y_5+Nty_5^2)\right] \\ y_7 \\ -\frac{Nt}{Nb}y_5'-Le[y_1 y_7-\gamma y_6] \end{pmatrix} \quad (35)$$

The boundary conditions

$$\begin{pmatrix} y_1(0) \\ y_2(0) \\ y_5(0) \\ y_6(0) \\ y_2(\infty) \\ y_4(\infty) \\ y_6(\infty) \end{pmatrix} = \begin{pmatrix} S \\ 1 \\ -Bi(1-y_4) \\ 1 \\ 0 \\ 0 \\ 0 \end{pmatrix}$$

3. Validation of Result

The analysis for the validation of result was achieved in table 2 which proved an excellent agreement with that of [1, 20, 21].

Table 2. *Evaluation for the outcomes of* $f''(0)$ *when* $\beta = Ra = S = Bi = \lambda = 0$ *and* $K \to \infty$, *with previous work.*

M	[20]	[21]	[1]	Present results
0.0	-1.00000	- 1.00000	-1.00000	-1.000000000
0.5	-1.224747	-1.224744	-1.224745	-1.224744871
1.0	-1.414217	-1.414213	-1.414215	-1.414213562

4. Results and Discussion

In this study, the default values are $Nr = \frac{1}{2}$, $N = \frac{1}{100}$, $S = \frac{1}{10}$, $Ra = \frac{1}{100}$, $Le = \frac{1}{5}$, $M = \frac{1}{5}$, $Nt = \frac{1}{5}$, $\gamma = \frac{1}{10}$, $\Pr = \frac{71}{100}$, $\lambda = \frac{1}{2}$, $Nb = \frac{1}{5}$, $k = \frac{1}{2}$, $\beta = \frac{1}{5}$, $Ct = \frac{1}{5}$, $Q = \frac{1}{100}$, $Bi = \frac{1}{10}$. Unless otherwise detailed.

Velocity Outline

However, figures 2 to 4 illustrates the upshot of velocity outline for different values of porosity parameter (K), Rayleigh number (Ra) and Jeffrey parameter (λ) respectively. By enhancing the values of porosity parameter (K), and Rayleigh number (Ra) the velocity of Jeffrey nanofluid goes up and the opposite direction is noticed for raising Jeffrey parameter (λ). The porosity parameter (K) makes a way for heat to flow out through the outer surface. As a result, the particles inside the fluid will turn out to be solid. Physically, the Rayleigh number (Ra) is the ratio of Buoyancy to the product of viscous and heat diffusion. An increase in the Jeffrey parameter (λ) signifies weaker retardation time.

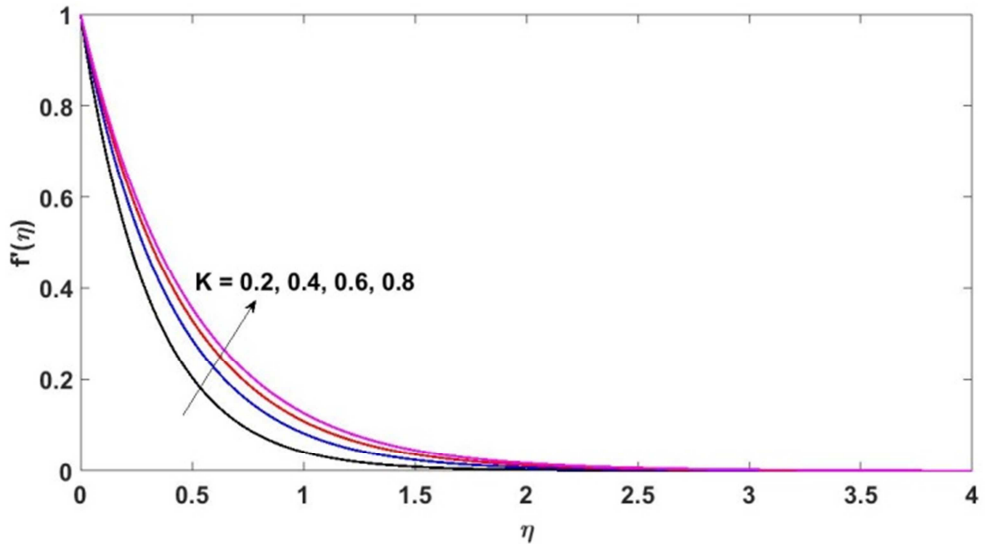

Figure 2. *Velocity profiles* $(f'(\eta))$ *for porosity parameter* (K).

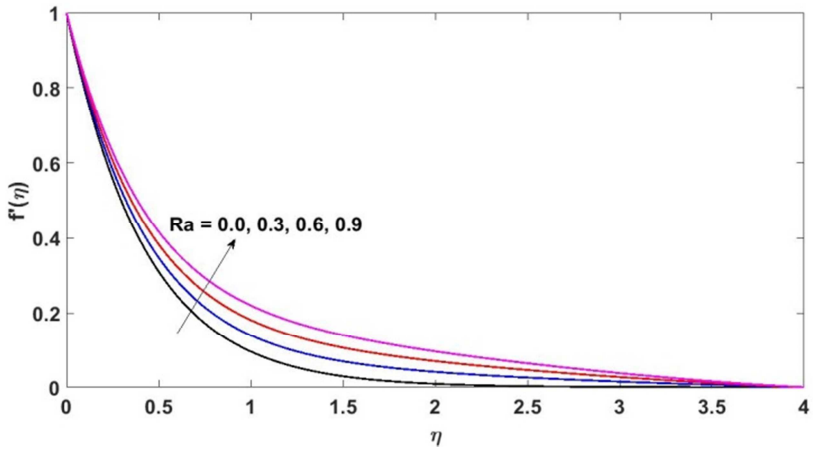

Figure 3. *Velocity profiles* $\left(f'(\eta)\right)$ *for Rayleigh number* (Ra).

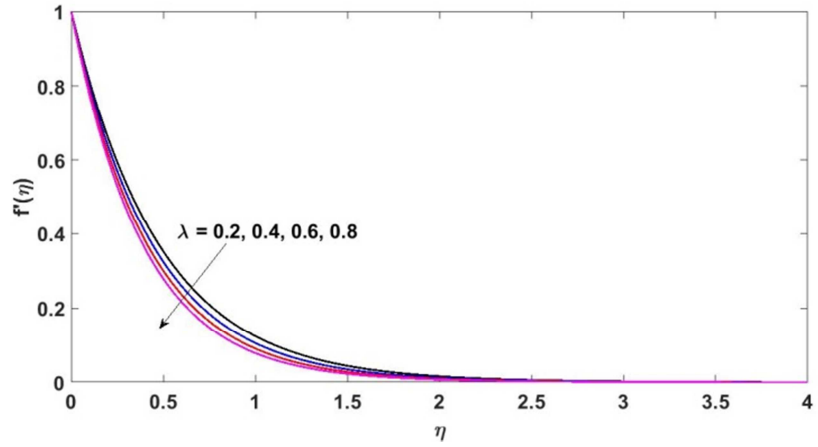

Figure 4. *Velocity profiles* $\left(f'(\eta)\right)$ *for Jeffrey parameter* (λ).

Temperature Outline

In addition, figures 5 to 7 displays the influence of temperature ratio (Ct), heat source-sink parameter (Q), and Prandtl number (Pr) on the temperature profile. The increase in temperature ratio (Ct) figure 5 and heat source-sink parameter (Q) figure 6 lead to an increase in the temperature profile while the temperature profile is depressed by enhancing the Prandtl number (Pr). Generally, more heat is produced by escalating the temperature ratio (Ct). The heat transfer occurrence is improved by an external heating source. Prandtl number (Pr) is the quotient of momentum to thermal diffusivity. The higher the heat transfers the greater the thermal diffusivity. It is used to calculate heat transmission between the exterior sheet and the fluid.

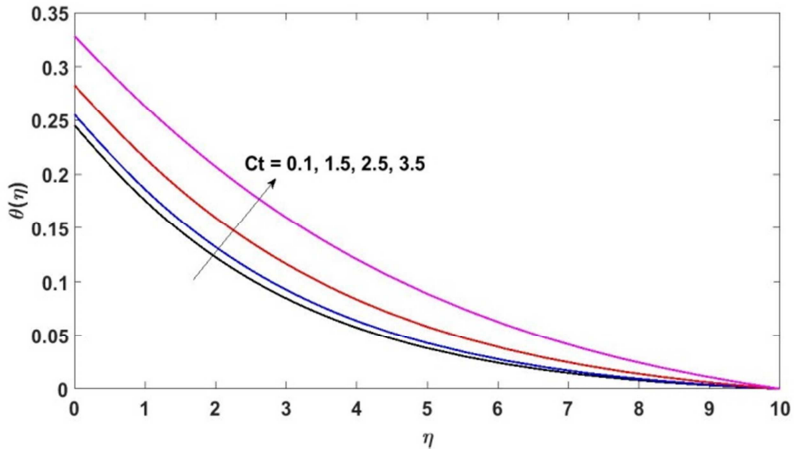

Figure 5. *Temperature profiles* $\left(\theta(\eta)\right)$ *for temperature ratio* (Ct).

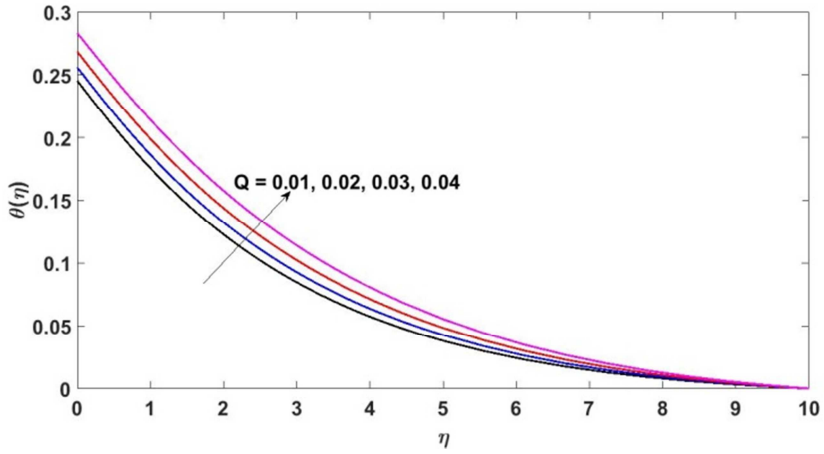

Figure 6. *Temperature profiles* $\left(\theta(\eta)\right)$ *for heat source-sink* (Q).

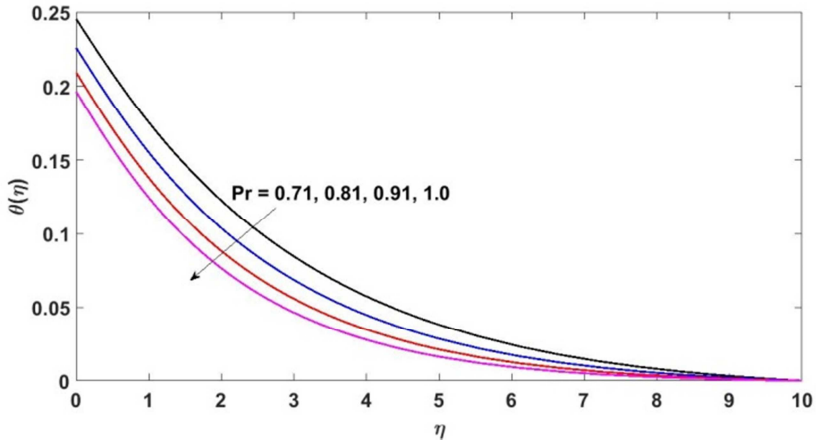

Figure 7. *Temperature profiles* $\left(\theta(\eta)\right)$ *for Prandtl number* (Pr).

Concentration Outline

Furthermore, figures 8 to 10 depict the upshots of concentration contour for diverse values of Lewis number (Le), chemical reaction parameter (γ), and Biot number (Bi) respectively. The concentration contour goes down by raising the values of the Lewis number (Le), and chemical reaction parameter (γ), and the reverse case for the Biot number (Bi). The Lewis number (Le) is a quotient of thermal diffusivity to the mass diffusivity. Biot number (Bi) signifies the quotient of conductive resistance in solids to the connective resistance in the thermal boundary layer.

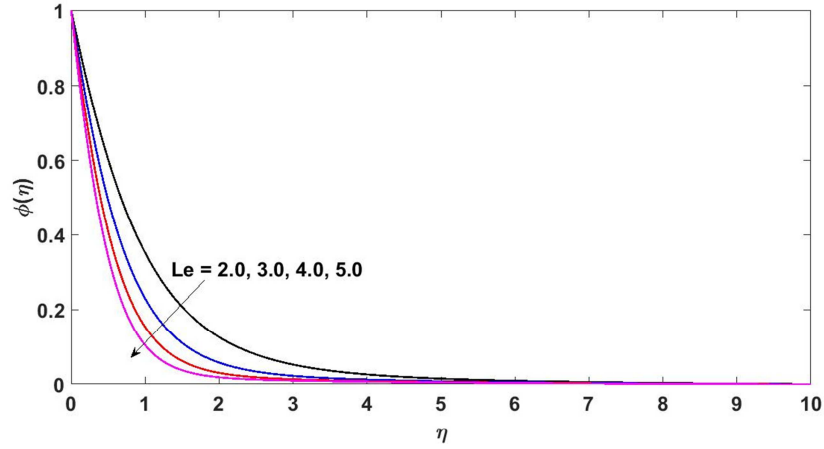

Figure 8. *Concentration profile* $\left(\phi(\eta)\right)$ *for Lewis number* (Le).

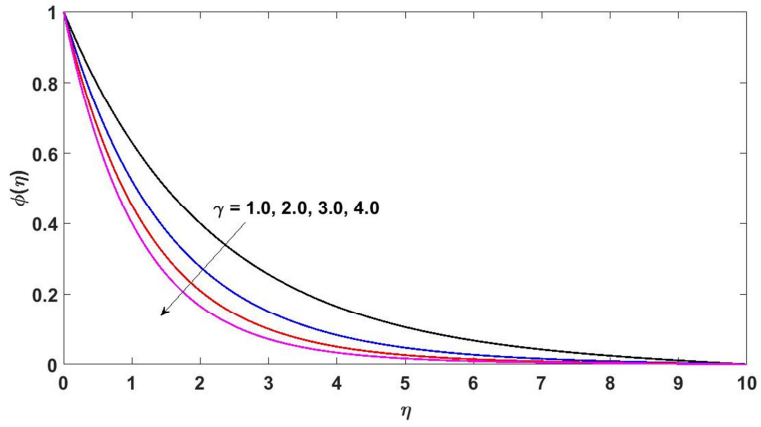

Figure 9. *Concentration profile* $(\phi(\eta))$ *for chemical reaction* (γ).

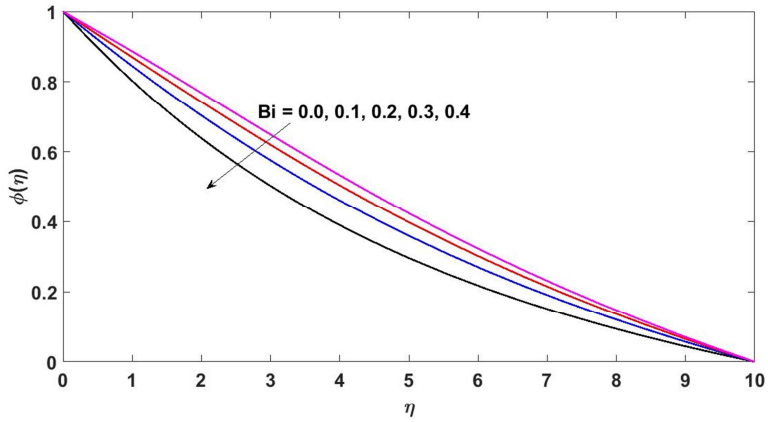

Figure 10. *Concentration profile* $(\phi(\eta))$ *for Biot number* (Bi).

Skin Friction Outline

Nevertheless, the influence of Jeffrey parameter (λ) and Hartmann number (M) on skin friction is disclosed in figure 11, 12 respectively. By boosting Jeffrey parameter (λ) and Hartmann number (M) the skin friction diminished. Generally, both Jeffrey parameter (λ) and Hartmann number (M) are reducing factor.

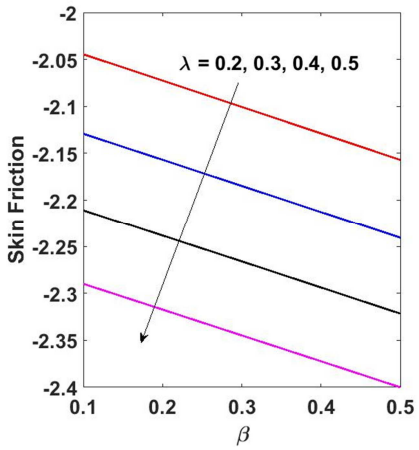

Figure 11. *Skin frictions for Jeffrey parameter* (λ)

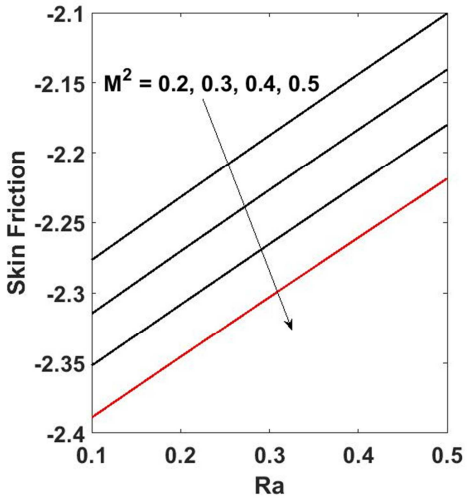

Figure 12. *Skin frictions for Hartmann number* (M).

Nusselt Number Outline

Also, the influence of Brownian motion (Nb) and Biot number (Bi) on Nusselt number is noticed in figures 13 and 14 respectively. By strengthen Brownian motion (Nb) the Nusselt number goes down whereas the opposite situation is noticed for the Biot number (Bi). This decline is due to the

nanoparticles of high thermal conductivity being determined from the warm area to the static liquid.

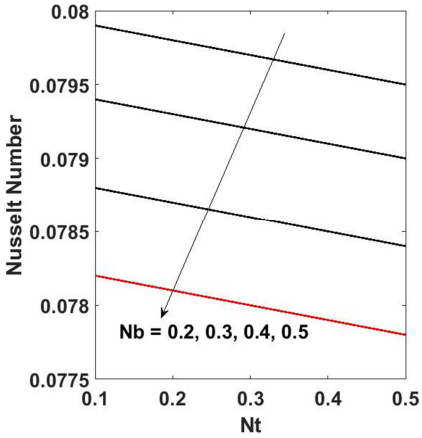

Figure 13. *Nusselt number for Brownian motion* (Nb).

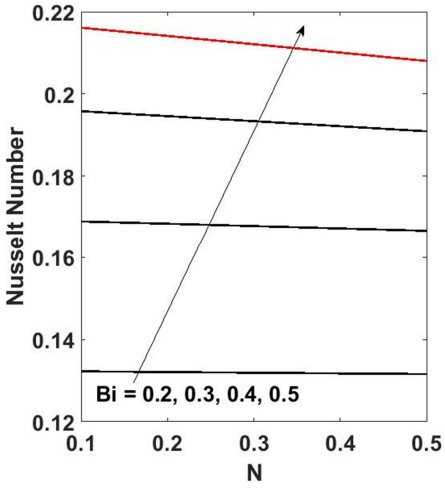

Figure 14. *Nusselt number for Biot number* (Bi)

Furthermore, the consequence of Brownian motion (Nb) and Biot number (Bi) on Sherwood number is noticed in figures 15 and 16 respectively. The Sherwood number goes up by enhancing Brownian motion (Nb) and takes the opposite direction for the Biot number (Bi).

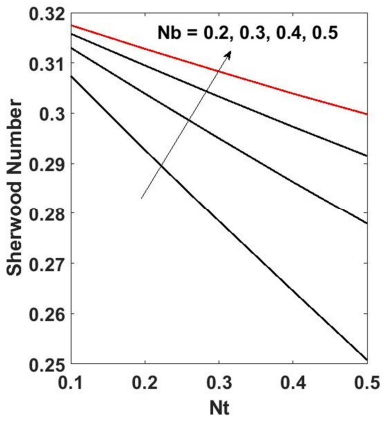

Figure 15. *Sherwood number for Brownian motion* (Nb).

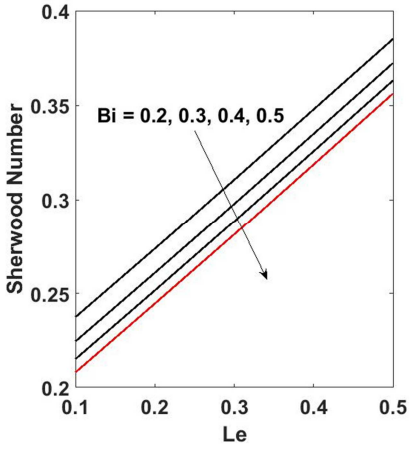

Figure 16. *Sherwood number for Biot number* (Bi).

5. Conclusion

The steady state heat and mass transfer in Jeffrey nanofluid with nonlinear thermal radiation was analyzed. The following are the major verdicts:

1. The velocity of the fluid is improved by strength of Rayleigh number (Ra) and porosity parameter (K)
2. The increase of thermal radiation parameter (N) and heat source-sink parameter (Q) in a Jeffrey nanofluid heats to an increase in the flow temperature and the opposite flow is noticed for the Prandtl number (Pr)
3. The concentration of the fluid goes down by growing Lewis number (Le) and chemical reaction (γ) and takes the opposite direction for Biot number (Bi)
4. The skin friction is diminished by enhancing Jeffrey parameter (λ) and Hartmann
5. Number (M)
6. The Nusselt number shrinks with raising Brownian motion (Nb) and takes opposite direction for Biot number (Bi)
7. The Sherwood number goes up by enhancing Brownian motion (Nb) and goes down by escalating the Biot number (Bi)

References

[1] B. Ahmad, A. Nawaz, S. U. Khan, M. I. Khan, T. Abbas, Y. D. Reddy, K. Guedri, M. Y. Malik, B. S. Goud, A. M. Galal, "Thermal diffusion of Maxwell nanoparticles with diverse flow features: Lie group simulations," *International Communication in Heat and Mass Transfer.* vol. 136, p. 106-164, 2022.

[2] B. K. Jha, and G. Samaila, "Nonlinear approximation for buoyancy-driven mixed convection heat and mass transfer flow over an inclined porous plate with Joule heating, nonlinear thermal radiation, viscous dissipation and thermophoresis effects," *Numerical Heat Transfer, Part B: Fundamentals,* 2022, DOI: 10.1080/10407790.2022.2150341.

[3] M. I. Khan, M. Waqas, T. Hayat, A. Alsaedi, M. I. Muhammad Imran Khan, "Significance of nonlinear radiation in mixedconvection flow of magneto Walter-B nanoliquid," *International Journal of Hydrogen Energy* vol. 42, 26408–26416, 2017.

[4] M. R. Ilias, N. S. Aidah Ismail, A. Raji, N. A. Rawi, S. Shafie, "Unsteady aligned MHD boundary layer flow and heat transfer of a magnetic nanofluids past an inclined plate," *International Journal Mechanical Engineering,* vol. 9, no. 2, p. 197-206, 2020.

[5] M. O. Lawal, K. B. Kasali, H. A. Ogunseye, M. O. Oni, Y. O. Tijani, Y. T. Lawal "On the mathematical model of Eyring–Powell nanofluid flow with non-linearradiation, variable thermal conductivity and viscosity," *Partial Differential Equations in Applied Mathematics,* vol. 5, p. 1-11, 2022.

[6] O. F. Bidemi and M. S. S. Ahamed "Soret and Dufour effects on unsteady casson magneto-nanofluid flow over an inclined plate embedded in a porous medium," *World Journal of Engineering,* https//dio. Org/10.1108/WJE-04-2018-0144, 2019.

[7] S. Aman, I. Khan, Z. Ismail, M. Z. Salleh, A. S. Alshomrani, M. S. Alghamdi, "Magnetic field effect on Poiseuille flow and heat transfer of carbon nanotubes along a vertical channel filled with Casson fluid," *AIP Advances,* vol. **7** no. 1, p. 1-18, 2017.

[8] S. Aman, I. Khan, Z. Ismail, M. Z. Sallah, I. Tlili "A new Caputo time fractional model for heat transfer enhancement of water based graphene nanofluid: An application to solar energy" *Results in Physics,* vol. 9, p. 1352-1362, 2018.

[9] Z. Abbas, S. Hussain, M. Y. Rafiq, J. Hasnain, "Oscillatory slip flow of Fe3O4 and Al2O3 nanoparticles in a vertical porous channel using Darcy's law with thermal radiation," *Heat Transfer,* 2020, https://doi.org/10.1002/htj.21771,.

[10] M. G. Sobamowo, "Combined effects of thermal radiation and nanoparticles on free convection flow and heat transfer of casson fluid over a vertical plate," *International Journal of Chemical Engineering,* 2018, https://doi.org/10.1155/2018/7305973.

[11] K. Das, A. Sarkar*y*, P. K. Kundu*z*, "Nanofluid Flow over a Stretching Surface in Presence of Chemical Reaction and Thermal Radiation: An Application of Lie Group Transformation," *Journal of Siberian Federal University. Mathematics & Physics,* vol. 10, no 2, p. 146–157, 2017.

[12] T. Muhammad, H. Waqas, U. Manzoor, U. Farooq, Z. F. Rizvi, "On doubly stratified bioconvective transport of Jeffrey nanofluid with gyrotactic motile microorganisms," *Alexandria Engineering Journal* vol. 61, p. 1571-1583, 2021.

[13] T. Hayat, S. Qayyum, A. Alsaedi, "Mechanisms of nonlinear convective flow of Jeffrey nanofluid due to nonlinear radially stretching sheet with convective conditions and magnetic field," *Results in Physics* vol. **7,** 2341–2351, 2017.

[14] M. G. Reddy, and O. D. Makinde, "Magnetohydrodynamic peristaltic transport of Jeffrey nanofluid in an asymmetric channel," *Journal of Molecular Liquids* vol. 223, p. 1242–1248, 2016.

[15] M. Waqas, S. A. Shehzad, T. Hayat, M. Ijaz Khan, A. Alsaedi, "Simulation of magnetohydrodynamic and radiation heat transport in convectively heated stratified flow of Jeffrey nanofluid." *Journal of Physics and Chemistry of Solids*, vol. 133, p. 45-51, 2019.

[16] F. M. Abbasi, S. Shehzad, A. T. Hayat1, M. S. Alhuthali, (2016) Mixed convection flow of Jeffrey nanofluid with thermal radiation and double stratification. *Journal of Hydrodynamic,* vol. 28, no. 5, p. 840-849, 2016.

[17] G. C. Rana, "Effects of rotation on Jeffrey nanofluid flow saturated by a porous medium" *Journal of Applied Mathematics and Computational Mechanics,* vol. 20 no. 3, p. 17-29, 2021.

[18] M. A. N. Zin, I. Khan, S. Shafie, A. S. Alshomrani, "Analysis of heat transfer for unsteady MHD free convection flow of rotating Jeffrey nanofluid saturated in a porous medium," *Result in Physics,* vol. **7**, p. 288-309, 2017.

[19] S. U. Khan, S. A. Shehzad," Flow of Jeffrey nanofluids over convectively heated oscillatory moving sheet with magnetic field and porosity effects," *Journal of Porous Media* vol. 23, no. 6, 907-922, 2020.

[20] T. Hayat, M. Mustafa, I. Pop, "Heat and mass transfer for Soret and Dufours effect on mixed convection boundary layer flow over a stretching vertical surface in a porous medium filled with a viscoelastic fluid" *Communication Nonlinear Science Numerical Simulation,* vol. 15, p. 1183-1196, 2010.

[21] M. Turkyilmazoglu," The analytical solution of mixed convection heat transfer and fluid flow of a MHD viscoelastic fluid over a permeable stretching surface," *International Journal mechical science,* vol. 77 p. 263-268, 2013.

[22] X. Y. Li, S. R. Mishra, P. K. Pattnaik, S. Baag, M. Y. Li, I. M. Khan, B. N. Khan, K. M. Alaoui, U.S. Khan, (2022) Numerical treatment of time dependent magnetohydrodynamic nanofluid flow of mass and heat transport subject to chemical reaction and heat source, *Alexendrial Engineering Journal.* 61: (3) 2484–2491.